The development of tea blister caused by Exobasidium vexans in tea (Camellia sinensis) correlates with the reduced accumulation of some antimicrobial metabolites and the defence signals salicylic and jasmonic acids

Mur, Luis; Hauck, Barbara; Winters, Ana; Heald, James Kevin; Lloyd, Amanda Jane; Chakraborty, U.; Chakraborty, B. N.

Published in:
Plant Pathology

DOI:
10.1111/ppa.12364

Publication date:
2015

Citation for published version (APA):
Mur, L., Hauck, B., Winters, A., Heald, J. K., Lloyd, A. J., Chakraborty, U., & Chakraborty, B. N. (2015). The development of tea blister caused by Exobasidium vexans in tea (Camellia sinensis) correlates with the reduced accumulation of some antimicrobial metabolites and the defence signals salicylic and jasmonic acids. *Plant Pathology*, *64*(6), 1471-1483. https://doi.org/10.1111/ppa.12364

Plant Pathology (2015) **64**, 1471–1483 Doi: 10.1111/ppa.12364

The development of tea blister caused by *Exobasidium vexans* in tea (*Camellia sinensis*) correlates with the reduced accumulation of some antimicrobial metabolites and the defence signals salicylic and jasmonic acids

L. A. J. Mur[a]*, B. Hauck[a], A. Winters[a], J. Heald[a], A. J. Lloyd[a], U. Chakraborty[b] and B. N. Chakraborty[b]

[a]*Institute of Biological, Environmental and Rural Sciences, Aberystwyth University, Edward Llwyd Building, Aberystwyth, SY23 3DA, UK; and* [b]*Department of Botany, University of North Bengal, Siliguri 734013, India*

Blister blight (causal agent, *Exobasidium vexans*) is an economically devastating disease of tea (*Camellia sinensis*). To determine what metabolite changes occur with tea blister that could be linked to disease progression, metabolomic approaches were used on *E. vexans* infected tea from a Darjeeling (India) plantation. Samples were classified according to disease phenotypes, i.e. either healthy or at one of three stages of disease progression. Initial metabolite fingerprinting using Fourier transform infrared (FTIR) spectroscopy indicated that metabolite changes could be related to disease stage. Electrospray ionization mass spectrometry (ESI-MS) highlighted caffeine and flavonoid metabolism changes as disease progressed. High-performance liquid chromatography (HPLC) with online photodiode array detection and electrospray ionization-tandem mass spectrometry (HPLC-PDA-ESI/MS^n) was used to characterize the caffeine, flavan-3-ol, flavone and flavonol profiles. There were increases in quercetin and kaempferol glucosides, kaempferol triglycosides and some catechin-class antioxidants, but also substantial reductions in apigenin and myricetin glycosides and, particularly, caffeine as disease progressed. The content of important defence hormones, salicylic acid and jasmonic acid, was also reduced in blister blight diseased samples. Thus, *E. vexans* infections perturb defence signalling and reduce many potentially antimicrobial compounds, such as caffeine, to aid disease progression.

Keywords: caffeine, catechins, flavonoids, tea blister disease

Introduction

Tea (*Camellia sinensis*) production is an important component of Indian agricultural production and gross domestic product (GDP). Indian tea accounts for 31% of global production with a total turnover of $1·8 billion, earning >$300 million dollars total net foreign exchange (FAOSTAT, 2010). Most Indian production is black tea where leaves are first rolled to break intracellular compartmentalization. Thus, phenol oxidases come into contact with phenolic compounds, allowing their oxidation to proceed for 90–120 min prior to drying. During this 'fermentative' period the distinctive black tea flavour begins to develop as flavan-3-ols condense to form theaflavins and their polymers thearubigins (Del Rio *et al.*, 2004). By contrast, in green tea production rolled leaves are immediately steamed so that flavan-3-ol oxidation does not take place.

*E-mail: lum@aber.ac.uk

Published online 11 March 2015

Given the economic importance of tea, any threats to yield are of great importance. Blister blight caused by *Exobasidium vexans* is a leaf disease in tea that preferentially attacks the economically important young leaves and is by far the most serious disease of cultivated tea (Punyasiri *et al.*, 2005). If not controlled by fungicides, tea losses due to blister blight may be as high as 35% (Radhakrishnan & Baby, 2004). *Exobasidium vexans* is an obligatory pathogenic basidiomycete spread by windborne basidiospores. Infection most likely proceeds through stomata (Punyasiri *et al.*, 2005) and on germination the mycelium grows intercellularly before the basidia fruiting bodies form below the lower epidermis. As these develop they force up and rupture the epidermis to form the blister (Boekhout, 1991). Macroscopically, *E. vexans* is typified by an initial discolouration of the infected leaf area before the formation of circular blisters (Punyasiri *et al.*, 2005).

The main control measure for blister blight is through the use of fungicides, particularly carbendazim, hexaconazole, propiconazole and tridemorph. These fungicides are applied every 2 weeks throughout the period when the disease is prevalent (Premkumar & Baby, 2005). This imposes a considerable additional financial cost and also logistical problems that could allow the blister blight

Plant Pathology

fungus to persist in tea plantations. Strategies of disease control based on host resistance mechanisms have been relatively unexplored (Martosupono, 1991). Some level of resistance to blister blight has been noted in tea cultivars (Balasooriya, 1996) with chitinase possibly playing a role in reducing blister formation (Jeyaramraja *et al.*, 2005), as may increases in polyphenol oxidase and peroxidase activities (Rajalakshmi & Ramarethinam, 2000).

Given the chemical richness of tea, resistance is also likely to depend on antimicrobial metabolites that need to be identified if they can be exploited in, for example, breeding programmes. The most abundant flavan-3-ols are (–)-epicatechin and gallic acid derivatives, but other important chemical classes include flavonols, such as conjugates of quercetin and kaempferol, coumarate, some purine alkaloids, theobromine and also the purine alkaloid, caffeine (Finger *et al.*, 1991, 1992; Kiehne & Engelhardt, 1996a,b; Kiehne *et al.*, 1997). Even a cursory examination of the literature from clinical microbiology shows that certain tea metabolites have antimicrobial activity (Park *et al.*, 2004; Song & Seong, 2007; Aron & Kennedy, 2008; Evensen & Braun, 2009; Sitheeque *et al.*, 2009; Gordon & Wareham, 2010) but there have been relatively few attempts to examine how such metabolites change during disease development. Preliminary studies have reported changes in saccharide metabolism (Pius *et al.*, 1998) and provided some evidence of antimicrobial phytoalexins, catechin and methylxanthine accumulation following infection by blister blight (Vidhyasekaran, 1988; Nagahaulla *et al.*, 1996; Rajalakshmi & Ramarethinam, 2000; Punyasiri *et al.*, 2005).

In this paper, metabolomic approaches are employed to begin to map changes in metabolites in young tea leaves as blister symptoms develop within a plantation. These could be sources of resistance or susceptibility that could be more fully characterized in subsequent studies. Major metabolite differences are described, centring on the reduced accumulation of caffeine and the important defence signals salicylic acid (SA) and jasmonic acid (JA) as well as apigenin and myricetin glycosides and increases in kaempferol and quercetin triglycosides. The importance to breeding programmes of screening for tea germplasm where the levels of these metabolites are maintained is discussed.

Materials and methods

Sampling tea from a Darjeeling plantation

All tea plants were of the North Indian Assam variety (TV-9) growing within Margaret's Hope Tea Gardens (North Kurseong, Darjeeling, India, 26·951° N, 88·280° E; altitude 950–1830 m a.s.l.). Natural infections of tea blister were sampled over a 4 h period and grouped into one of four disease stage classes (Fig. 1). These classes represented apparently uninfected healthy (H) young leaves of tea (Fig. 1a), early symptoms of *E. vexans* infection consisting of a reddening at the infection site (Fig. 1b; designated infection stage 1; S1), samples exhibiting the formation of characteristic blisters (Fig. 1c; infection stage 2; S2) and samples where blisters had led to the formation of large necrotic patches in the leaves (Fig. 1d; infection stage 3; S3).

Samples were collected from 10 geographical sites within the Margaret's Hope Tea Gardens (in this paper designated a to j) of approximately 20 m^2 each and separated from each other by at least 100 m. Plants were sampled between 10:00 and 14:00 h on 15 and 16 June. At each site samples of 10 leaves at each infection stage as well as healthy (symptomless) controls were taken and separately pooled. Thus, four pooled samples of each phenotypic class were taken so that a total of 40 samples (10 of each phenotypic class) were taken forward for metabolomic analyses.

Sample preparation

Samples were taken from the plantation on wet ice and processed on the day they were sampled. A total of 5 g from each sample pool was ground to a fine powder in liquid nitrogen. The metab-

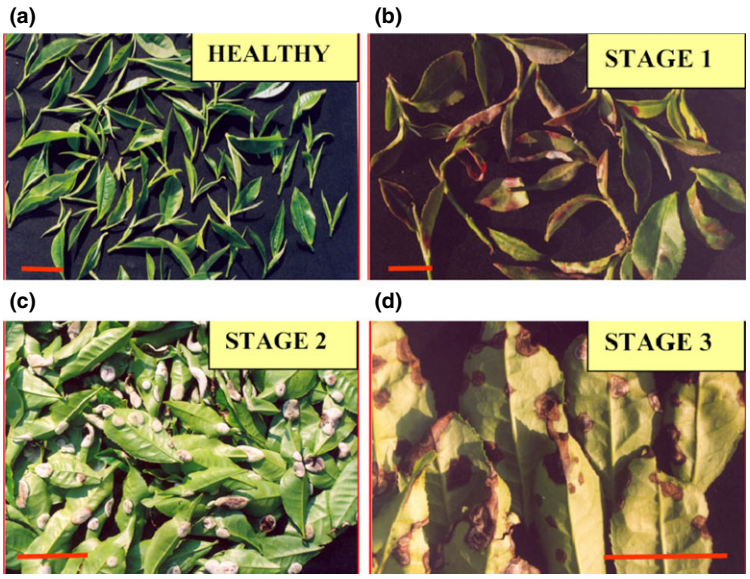

Figure 1 Stages of blister blight disease on tea (*Camellia sinensis*) leaves. Healthy leaves (a) and tea leaves infected with tea blister blight (*Exobasidium vexans*) at designated infection stages 1 (b), 2 (c) and 3 (d). Bar = 1 cm.

olites were extracted using a 10 mL chloroform:methanol:water (22:56:22) mix which allowed the isolation of both polar and nonpolar metabolites. The slurry was centrifuged at 3400 *g* to remove any particulate matter and the supernatants collected. The volatile components of the extraction mix were evaporated over a waterbath at 45°C for 4–6 h as required. The aqueous solvent was removed by lyophilization. The dried samples were then dispatched to Aberystwyth University in the UK. On receipt, the samples were resuspended in 1 mL methanol:water (70:30) and stored at −80°C until analysis within a month of receipt.

Fourier transform infrared (FTIR) spectroscopy

This was undertaken in accordance with the manufacturer's instructions (Bruker BioSciences Corp.) and as described in Johnson *et al.* (2003). Spectra were created over a wavenumber range of 4000 to 600 cm^{-1} using 64 co-added scans at 4 cm^{-1} resolution, permitting collection of 1763 data points. Data were analysed using MATLAB v. 6.5 (The MathWorks, Inc.) or PYCHEM (Jarvis *et al.*, 2006). In-house algorithms were used to convert the resultant spectra into absorbance. CO_2 peaks were replaced with a smooth trend using an in-house code and the spectra were normalized to total absorbance (Timmins *et al.*, 1998).

Direct injection electrospray ionization-mass spectrometry (DI-MS)

Direct injection electrospray ionization-mass spectrometry was carried out using a Micromass LCT mass spectrometer (Micromass/Waters Ltd) in negative ionization mode, which has been shown to be effective for characterization of plant extracts (Mattoli *et al.*, 2006). Extracts were reconstituted in 0·25 mL 30% (v/v) methanol:H_2O. Extracts of 10 μL were introduced by DI at a flow rate of 0·5 mL min^{-1} in 30% (v/v) methanol:H_2O running solvent, using a Harvard 11 syringe pump (Harvard Ltd). Direct injection electrospray ionization-mass spectrometry data were acquired over the *m/z* range of 100–1400 and were imported into MATLAB, binned to unit mass and then normalized to percentage total ion as stated in Johnson *et al.* (2007).

Liquid chromatography

Typically, 50 μL of extract were analysed by reverse-phase HPLC on a Waters system with a 996 photodiode array detector (PDA) and a Nova-Pak C_{18} radial compression column (4 μm, 8 × 100 mm; Waters Ltd). The column was equilibrated with 100% solvent A (5% acetic acid) at a flow rate of 2 mL min^{-1}. Metabolites were eluted from the column by linear gradient to 100% solvent B (100% methanol) over 50 min and monitored from wavelengths of 240 to 400 nm.

Liquid chromatography mass spectrometry (LC-MS)

Compounds within selected samples were tentatively identified by reverse-phase high performance liquid chromatography (HPLC) with an online photodiode array (PDA) detector and electrospray ionization-tandem mass spectrometry (HPLC-PDA-ESI/MS^n). Analyses were performed on a Thermo Finnigan system (Thermo Electron Corp.) comprising a Finnigan Surveyor PDA Plus detector, a Finnigan LTQ linear ion trap with ESI source and a Waters Nova-Pak C_{18} column (4 μm, 3·9 × 100 mm). The autosampler tray temperature was maintained at 5°C and the column temperature at 30°C. Sample injection volume was typically 10 μL, the detection wavelength was set to 240–400 nm, and the flow rate was 1 mL min^{-1} with 10% of the sample going to the mass spectrometer (MS). The mobile phase consisted of water/0·1% formic acid (solvent A) and methanol/0·1% formic acid (solvent B). The column was equilibrated with 95% A, and the percentage of B increased linearly to 55% over 50 min. Interface and MS parameters were optimized by infusion of chlorogenic acid standard at a constant rate into the LC flow. Mass spectra were acquired in negative and positive ionization mode with the following parameters: nitrogen sheath gas 30 arbitrary units, nitrogen auxiliary gas 15 arbitrary units and capillary temperature 320°C. Spray voltage was 4·0 kV in negative ionization mode and 4·8 kV in positive ionization mode, capillary voltage –1 V and 45 V, respectively, and tube lens offset –68 V and 110 V. MS/MS fragmentation was carried out at normalized collision energy of 35% and isolation width 2·0 (*m/z*). For analysis of flavan-3-ols, ionization parameters were optimized further by infusion of catechin standard (Sigma-Aldrich) into the LC flow.

Naringinase assays

To identify sugar moieties in flavonoid glycosides, selected extracts were treated with naringinase from *Penicillium decumbens* (Sigma Aldrich), an enzyme with glucosidase and rhamnosidase activity. Naringinase (399 U enzyme activity per gram solid) was made up in McIlvaine buffer, pH 4·0, at 17 U mL^{-1}. Assays were carried out in McIlvaine buffer, pH 4·0, with 50 μL of extract and an enzyme concentration of 6·7 U mL^{-1} in a total volume of 1·5 mL. After incubation for 2·5 h at 40°C, samples were partially purified on a 500 mg Sep-Pak C_{18} 3 cc Vac RC cartridge (Waters) following the manufacturer's instructions, dried down at 50°C under nitrogen and redissolved in 70% methanol for analysis by LC-MS.

To confirm the identity of flavonol aglycones, 100 μL of selected extracts were hydrolysed in a total volume of 1 mL 1 M HCl. Following incubation for 1 h at 100°C, the pH of the samples was adjusted to 4·5. Extracts were then partially purified on a 500 mg Sep-Pak C_{18} 3 cc Vac RC cartridge, dried down at 50°C under nitrogen and redissolved in 70% methanol for analysis by LC-MS.

Data analysis

Principal component analysis (PCA) and discriminant function analysis (DFA) based on principal components (PCs) were used as described in Allwood *et al.* (2006) and followed accepted MSI standards (Goodacre *et al.*, 2007). Principal component analysis reduces the dimensionality of multivariate data whilst preserving most of the variance, following which DFA is used to discriminate between groups on the basis of the retained PCs and the a priori knowledge of class structures within the data sets. All calculations were performed in MATLAB or PYCHEM. The major sources of variation were targeted from the loading vectors (eigenvalues), which contributed > ± 2 standard deviations to the observed variation. KEGG (http://www.genome.jp/kegg/) and the Sheffield tomato ESI (http://aps.group.shef.ac.uk/tomato/index.html) metabolite databases were used to assign a tentative identification to each *m/z* value.

Heat maps were generated using EPCLUST software (Brazma *et al.*, 2003). Comparisons of the metabolite peaks from different treatments with controls were performed using Tukey multiple pairwise comparison test using MINITAB v. 14 (Minitab Ltd). Differences with $P < 0·05$ were considered significant.

Salicylic acid and jasmonic acid measurements

Salicyclic and jasmonic acid concentrations in samples were determined by LC-MS using the Micromass LCT-time of flight (LCT-ToF), as described in Clarke *et al.* (2004) and Allwood *et al.* (2006), respectively. Absolute SA and JA concentrations were derived by comparison with deuterated standards (d_6-SA (C/D/N Isotopes Inc.); d_6-JA standard, kindly provided by Claus Wasternack (Leibniz Institute of Plant Biochemistry, Halle, Germany)), which were added to the samples at first extraction.

Results

Fourier transform infrared fingerprinting

Extracts from young healthy tea leaves (Fig. 1a) and tea blister-exhibiting leaves at each designated stage of infection (Fig. 1b, c, d) were investigated using FTIR spectroscopy. The derived spectra indicated that the plantation-sourced samples were chemically rich but infection-specific changes could not be observed without mathematical analyses (Fig. 2a). Employment of the supervised DFA, which employs a priori knowledge of the experimental class, showed clustering according to stage of disease, of healthy samples (H), a group comprising of S1 and S2 infection stages, and most clearly the necrotic infection stage 3 (Fig. 2b).

The data were further investigated by employing DFA to assess how far infection could dominate over biochemical variation linked to sampling site (Fig. 2c, d). DFA suggested that there were some biochemical differences of the FTIR spectra of Stage 1 samples from those of the healthy controls, but these were difficult to distinguish from the variation due to sampling site (Fig. 2c). However, with the blister stage 2 samples, they were clearly separated from H samples along the DF1 axis, indicating infection-associated changes that could not be linked to sampling site (Fig. 2d).

Tentative identification of the main metabolite changes following infection with *E. vexans*

Direct injection electrospray ionization-mass spectrometry was employed for metabolite profiling and tentative indications of the changes that occurred following

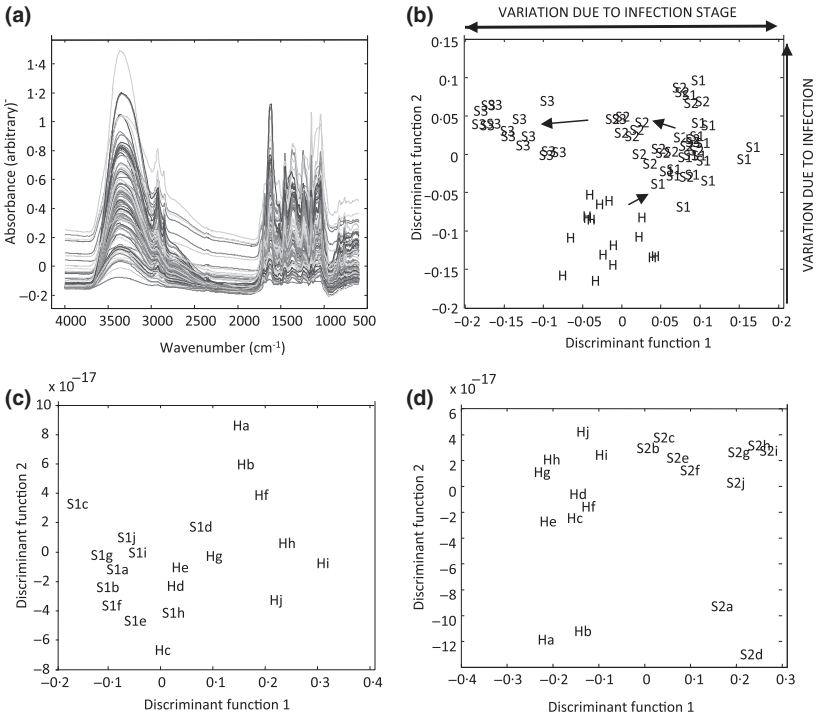

Figure 2 FTIR analysis of tea leaves infected with tea blister blight (*Exobasidium vexans*) sampled from Margaret's Hope Tea Gardens, Darjeeling, India. (a) FTIR spectra derived from healthy and blister blight infected tea leaves at designated infection stages. (b) Discriminant function analysis (DFA) of 10 samples from each biological class: H = healthy; S1 = stage 1; S2 = stage 2; and S3 = stage 3. The model is based on 10 principal components (PC) that encompassed 99·23% of the total variance amongst the samples. Discriminant function (DF) axes discriminating metabolite differences at different stages of infection (Discriminant Function 1) and changes associated with infection (Discriminant Function 2) are indicated. The arrows are included to highlight changes according to infection stage and have no mathematical relevance. (c) DFA of samples from healthy and stage 1 infected leaves. The model is based on 10 PCs that encompassed 97·56% of the total variance amongst the samples. (d) DFA of samples from healthy and stage 2 infected leaves. The model is based on 10 PCs that encompassed 98·78% of the total variance amongst the samples. In (c) and (d) the a to j suffixes refer to one of 10 different locations within the Margaret's Hope Tea Gardens.

infection were derived. Spectra derived following DI-MS in negative ionization mode (ESI^-) were analysed by DFA. As with the analyses of FTIR spectra, stages S1 and S2 were readily separated from healthy samples, with S3 forming a distinct group (Fig. 3a). Metabolite differences between healthy and stage 1 disease were focused on because they encompassed the earliest infection events and so minimized the potential contribution of metabolites from the fungus. DFA of spectra only from healthy and stage 1 disease samples included the site of origin classifications (Fig. 3b). This readily discriminated between healthy and stage 1 samples, overriding any site-specific influences, with the major sources of variation separating along the DF1 axis. The PC-DF1 loadings (eigenvalues), indicating the relative value of each mass-ions (*m/z*) in contributing to the separation seen in DF1 (Fig. 3b), were plotted (Fig. 3c) and the major sources of variation (32 *m/z*) were identified. When DFA was undertaken using data for these 32 *m/z* values, good separation between stage 1 and healthy samples was maintained (Fig. 3d). The list of tentatively identified *m/z* (Table 1) suggested many metabolites from the caffeine biosynthetic pathway (Fig. S1) and flavonoid pathways leading to the production of certain flavan-3-ol and flavonols (Fig. S2).

Targeting caffeine and flavonoid changes in *E. vexans*-challenged tea

To focus on potential changes in caffeine and flavonoids, samples were analysed by HPLC-PDA with detection at 280 nm (targeting caffeine and flavan-3-ols) and 340 nm (targeting flavones and flavonols). Example chromatograms for healthy and each disease stage (S1, S2 and S3) are shown in Figure 4. For each wavelength the peaks in the chromatograms were aligned and designated according to retention times (Fig. 4; Tables 2 & 3).

Individual metabolites were characterized by HPLC-PDA-ESI/MS^n. Some compounds were readily identified by direct comparison of their retention times, UV spectra and fragmentation patterns with those of standards. Tentative identifications of other compounds were based on the similarity of their UV and MS spectra to known compounds and reports in the literature, following the principles outlined by Markby *et al.* (1970) and Vukics & Guttman (2010).

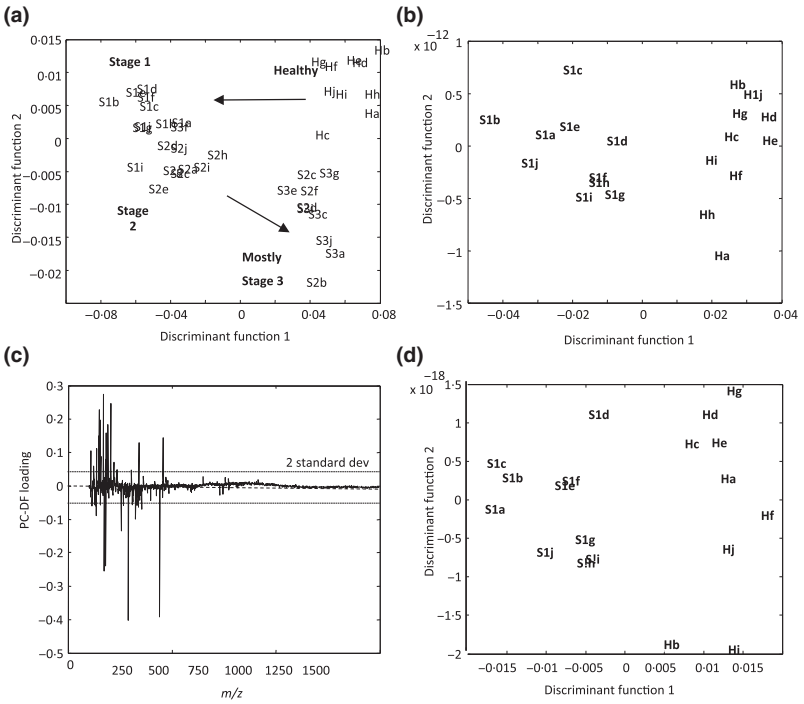

Figure 3 Multivariate analyses of metabolic profiles generated by electrospray ionization mass spectrometry (ESI-MS) of tea leaf samples infected with blister blight. (a) Discriminant function analysis (DFA) of samples from healthy and tea blister blight infected tea leaves at designated infection stages, sampled at one of 10 sites within the Margaret's Hope Tea Gardens. H = Healthy; S1 = stage 1; S2 = stage 2; and S3 = stage 3. The model is based on 10 principal components (PC) that explained 98·39% of the total variance amongst the samples. The arrows are included to highlight changes according to infection stage and have no mathematical relevance. (b) DFA of samples from healthy and stage 1 infected leaves. The model is based on 10 PCs that encompassed 95·89% of the total variance amongst the samples. (c) A plot of the loading vectors linked to *m/z* associated with Discriminant Function 1 shown in (b). (d) DFA of sub-matrix of the top 32 discriminatory *m/z* as indicated from the loading vector plot (c). The model is based on four PCs that encompassed 99·02% of the total variance amongst the samples in (b) and (d). Suffixes a to j refer to one of 10 different locations within the Margaret's Hope Tea Gardens.

Table 1 Tentative identifications of the *m/z* from electrospray ionization mass spectrometry (ESI-MS) of tea samples exhibiting blister blight

m/z (−H)	True mass	Tentative identity
109	110	Catechol
117	118	Succinate
117	306	Epigallocatechin, leucocyanindin
128	129	?
128	316	Isorhamnetin
132	133	Asparate
135	136	Hypoxanthine
137	138	Salicylic acid
145	146	α-Ketoglutamate
151	152	Xanthine
164	165	Phenylalanine
169	170	Gallic acid
173	174	Shikimic acid
179	180	Jasmonic acid
193	194	Caffeine
225	226	Chorismate
279	280	Linolenic acid
286	287	Cyanidin
287	288	Dihydrokaempferol
289	290	Epicatechin
289	290	(9Z,15Z)-(13S)-12,13-Epoxyoctadeca-9,11, 15-trienoic acid
293	294	8-[(1R,2R)-3-oxo-2-{(Z)-pent-2-enyl} cyclopentyl]octanoate
325	326	?
331	332	β-Glucogallin
339	340	Glucose/fructose 1,6-bisphosphate
353	354	Chlorogenic acid
397	398	S-adenosyl-L-methionine
457	458	Epigallocatechin gallate
458	459	?
471	472	?

Compounds detected at 280 nm included caffeine, gallic acid derivatives and flavan-3-ols (Table 2), which are commonly observed constituents in tea (Friedman *et al.*, 2005; Lin *et al.*, 2008; Wang *et al.*, 2008). Compounds 8A, 4, 6, 7 and 8B were readily identified as caffeine, catechin, epigallocatechin gallate, epicatechin and gallocatechin gallate, respectively, by comparison with reference compounds. Compound 5 with M_r 306 Da showed the same UV spectrum and fragmentation pattern as gallocatechin standard but eluted at a different retention time and was tentatively identified as epigallocatechin.

The characteristics of compound 1 were consistent with gallate (Del Rio *et al.*, 2004), whereas compound 3 (M_r 184 Da) with an MS^2 base peak at *m/z* 168 in negative ionization mode (–15 Da), indicating loss of a methyl group, was tentatively identified as methyl gallate. Fragmentation of the peak 2 parent ion at *m/z* 343 in negative mode produced ions with *m/z* 191 and 169. Subsequent MS^3 analysis of the ion at *m/z* 191 produced fragments also observed for quinate standard, while the ion at *m/z* 169 yielded a fragment with *m/z* 125, consistent with gallate, and compound 2 was therefore identified as galloyl quinate. The fragmentation pattern of peak 10 with *m/z* 441 was similar to that reported for epicatechin-3-gallate (Del Rio *et al.*, 2004; Lu *et al.*, 2009), and MS^3 analysis of the main MS^2 fragments with *m/z* 289 and *m/z* 169 yielded ions characteristic for epi/catechin (*m/z* 245, 205 and 179) and gallate (*m/z* 169), respectively, supporting the identification of this compound as epi/catechin gallate. Similarly, compounds 9 (M_r 472 Da) and 11 (M_r 456 Da) showed fragmentation patterns consistent with flavan-3-ol methyl gallates and were identified as epi/gallocatechin methyl gallate and epi/catechin methyl gallate, respectively, which are less common constituents of tea leaves (Sano *et al.*, 1999; Wang *et al.*, 2008).

Based on their UV spectra and MS fragmentation patterns, the main peaks detected in the 340 nm chromatograms, listed in Tables 3 and 4, were classified as flavones (compounds 12, 13, 14B, 15, 16A, 17 and 20B), flavonols (compounds 14A and 14C, 16B, 18–20A and 21–24) and acylated flavonoids (25–28). Where UV spectra were convoluted considerably by co-eluting compounds, they were marked as not detected (nd) in Table 3.

All the flavones detected in the extracts were apigenin glycosides, and compounds 15 and 17 were identified as vitexin (apigenin-8-*C*-glucoside) and isovitexin (apigenin-6-*C*-glucoside), respectively, by direct comparison with standards. Compounds 12 (M_r 594 Da), 13 and 14B (both with M_r 564 Da) exhibited fragmentation patterns consistent with apigenin-*C*-diglycosides (Ferreres *et al.*, 2003, 2008; Wu *et al.*, 2004), whilst the fragmentation patterns of compounds 16A (M_r 594 Da) and 20B (M_r 578 Da) were consistent with apigenin-*C*-hexoside-2″-*O*-glycosides (Ferreres *et al.*, 2007), a conclusion substantiated further by the decrease of compounds 16A and 20B and an increase of vitexin and isovitexin in extracts treated with naringinase (data not shown). UV and MS spectra of the flavonol glycosides revealed a range of quercetin (compounds 16B, 18–20A and 21), kaempferol (compounds 22–24) and myricetin-*O*-glycosides (compounds 14A and 14C).

The peaks eluting between 28 and 32 min (Table 4) were classified as acylated flavonol glycosides, which are characterized by a broad UV absorbance band I that is shifted to a shorter wavelength (Santos-Buelga *et al.*,2003), with an absorbance maximum at around 317 nm indicating the presence of *p*-coumaroyl residues (Saracini *et al.*, 2005). Consecutive fragmentation of the parent ions and subsequent product ions revealed kaempferol and quercetin as aglycone cores. Losses of 162/180 Da were attributed to hexosyl residues and of 132/150 Da to pentosyl residues, whilst a loss of 146/164 Da could be accounted for by either a rhamnosyl or a *p*-coumaroyl residue. Based on the UV absorbance spectra it was concluded that each compound was conjugated with at least one *p*-coumarate moiety.

The range of compounds, including acylated flavonol glycosides, observed here has previously been reported in tea (Atoui *et al.*, 2005; Dou *et al.*, 2007; Lin *et al.*, 2008), and the fragmentation patterns observed for the acylated kaempferol conjugates are in agreement with

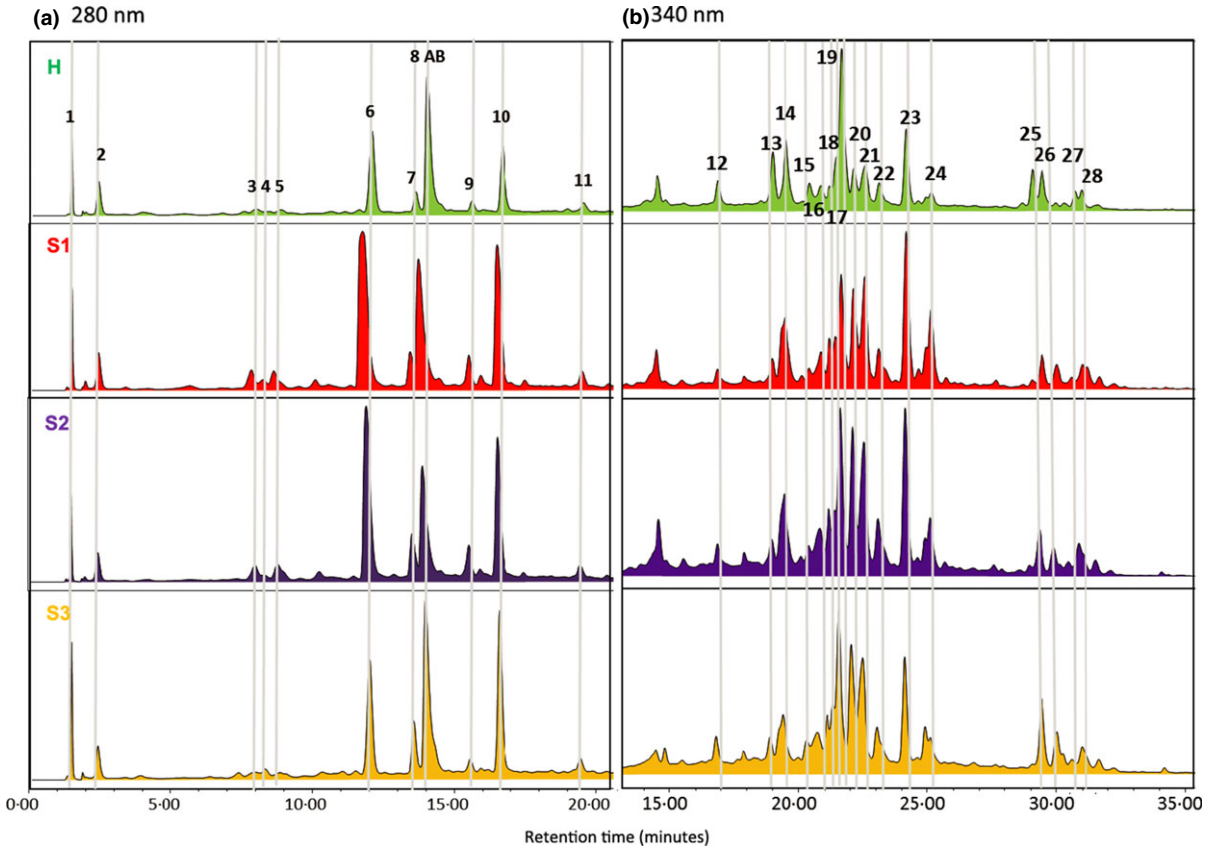

Figure 4 UV/vis chromatograms of samples representative of each blister blight disease stage. Representative UV/vis chromatograms at (a) 280 nm and at (b) 340 nm. Chromatograms of healthy tissue are shown in green (H), disease stage 1 in red (S1), disease stage 2 in purple (S2) and disease stage 3 in yellow (S3). Each selected peak is indicated by grey shading and designated by a number.

Table 2 Identification of metabolites detected in UV/vis chromatograms at 280 nm

Peak	RT (min)[a]	λ_{max} (nm)[b]	$[M - H]^-$ (*m*/*z*)[c]	$[M + H]^+$ (*m*/*z*)[d]	MS^2 fragment ions (*m*/*z*)	Tentative identification
1	1·5	275	169		125	Gallate
2	2·4	272	343		191, 169	Galloyl quinate
3	8·0	275	183		168, 124	Methylgallate
4	8·3	279	289		245, 205, 179	Catechin[e]
5	8·8	271	305		179, 221, 219, 261, 165, 125, 137, 247, 287	Epigallocatechin
6	12·0	274	457		169, 331, 305, 287	Epigallocatechin gallate[e]
7	13·5	279	289		245, 205, 179	Epicatechin[e]
8A	13·9	273		195	138	Caffeine[e]
8B	14·3	275	457		169, 331, 305, 287	Gallocatechin gallate[e]
9	15·5	277	471		183, 305, 287, 168	Epi-/gallocatechin methylgallate
10	16·5	278	441		289, 169, 331, 271	Catechin/epicatechin gallate
11	19·5	276	455		289, 183	Catechin/epicatechin methylgallate

[a]RT, retention time.
[b]Wavelength at which the maximum fraction of light is absorbed.
[c]Negative ionization of a mass-ion.
[d]Positive ionization of a mass-ion.
[e]Identified by direct comparison with standard.

Table 3 Identification of metabolites detected in UV/vis chromatograms at 340 nm

Peak	RT (min)[a]	λ_{max} (nm)[b]	$[M-H]^-$ (*m/z*)[c]	Main MS^2 fragment ions in negative mode	Main MS^2 fragment ions in positive mode	Tentative structure assignment
12	17·2	nd	593	473, 503, 353, 383, 575		Apigenin-6,8-di-*C*-hexoside
13	19·3	271, 337	563	473, 443, 503, 383, 353, 545, 425		Apigenin-6-*C*-pentoside-8-*C*-hexoside
14A	19·8	nd	479	316, 317		Myricetin-*O*-glucoside[d]
14B		nd	563	443, 473, 353, 383, 545, 503		Apigenin-6-*C*-hexoside-8-*C*-pentoside
14C		nd	625	316, 317	319, 481	Myricetin-*O*-glucosyl-rhamnoside[d]
15	20·7	269, 339	431	311, 341		Vitexin[e]
16A	21·1	270, 336	593	413, 293, 473, 341	433, 415, 367	Apigenin-*C*-hexoside-2″-*O*-glucoside[d]
16B		nd	771	301, 609	303, 611, 465, 449	Quercetin-*O*-hexoside-*O*-hexosyl-rhamnoside
17	21·5	271, 339	431	311, 341, 413		Isovitexin[e]
18	21·7	nd	463	301, 300		Quercetin-*O*-glucoside[d]
19	21·9	257, 355	771	301, 300, 609	303, 611, 465, 449	Quercetin-*O*-hexoside-*O*-hexosyl-rhamnoside
20A	22·4	258, 352	463	301, 300		Quercetin-3-*O*-glucoside[d]
20B		269, 345	577	413, 293, 457, 341	433, 415, 313	Apigenin-*C*-hexoside-2″-*O*- rhamnoside
21	22·8	257, 357	609	301, 300, 302	303, 465	Quercetin-3-*O*-glucosyl-rhamnoside[d]
22	23·4	266, 347	755	285, 593	287, 595, 449, 433, 577, 611	Kaempferol-*O*-hexoside-*O*-hexosyl-rhamnoside
23	24·4	266, 348	755	285, 593	287, 595, 449, 433	Kaempferol-*O*-hexoside-*O*-hexosyl-rhamnoside
24	25·4	266, 349	593	285	287, 449	Kaempferol-3-*O*-glucosyl-rhamnoside[d]

nd, not determined.

The identity of the flavonol moieties of *O*-glycosides was confirmed by comparison of the relevant MS^3 spectra in negative ionization mode to those of authentic aglycone standards.

[a]RT, retention time.

[b]Wavelength at which the maximum fraction of light is absorbed.

[c]Negative ionization of a mass-ion.

[d]Presence of glucosyl/rhamnosyl moiety confirmed by naringinase assay.

[e]Identified by direct comparison with standard.

Table 4 Characterization of acylated flavonol-glycosides detected at 340 nm

Peak	RT (min)[a]	λ_{max} (nm)[b]	$[M-H]^-$ (*m/z*)[c]	Flavonol core	Number and type of residues attached
25	29·2	258(sh), 268, 316	1079	Quercetin	2 *p*-Coumarate/rhamnose[d] 3 hexose
26	29·6	257(sh), 268, 317	1049	Quercetin	2 *p*-Coumarate/rhamnose[d] 1 pentose 2 hexose
27A	30·9	268, 317	1063	Quercetin	3 *p*-Coumarate/rhamnose[d] 2 hexose
27B			1063	Kaempferol	2 *p*-Coumarate/rhamnose[d] 3 hexose
28A	31·1	268, 317	1033	Quercetin	3 *p*-Coumarate/rhamnose[d] 1 pentose 1 hexose
28B			1033	Kaempferol	2 *p*-Coumarate/rhamnose[d] 1 pentose 2 hexose

sh, peak shoulder.

[a]RT, retention time.

[b]Wavelength at which the maximum fraction of light is absorbed.

[c]Negative ionization of a mass-ion.

[d]At least one is *p*-coumarate.

structures proposed by (Lee *et al.*, 2008) based on nuclear magnetic resonance (NMR) studies of similar compounds.

Changes in caffeine and flavonoids in *E. vexans*-challenged tea

Based on the peak areas, a data matrix was constructed for each wavelength (280 nm or 340 nm) and analysed using DFA. Initial analyses focused on the possible site-specific effects by comparing variation within the H samples (Fig. S3). These suggested that for metabolites detected at 280 nm, site j was distinctive, but for metabolites detected at 340 nm, site c displayed distinctive profiles. Apart from these two sites, the other sites were notable for the relative lack of variation.

Analysis of the 280 nm peak matrix indicated that there was considerable variation amongst the healthy samples, but these were distinct from diseased samples (Fig. 5a). Samples from S1 and S2 but not S3 formed a distinctive group that exhibited some limited separation along DF2. Examination of the loading vectors describing the variation along DF1, which separated between infected and healthy samples, indicated a particular

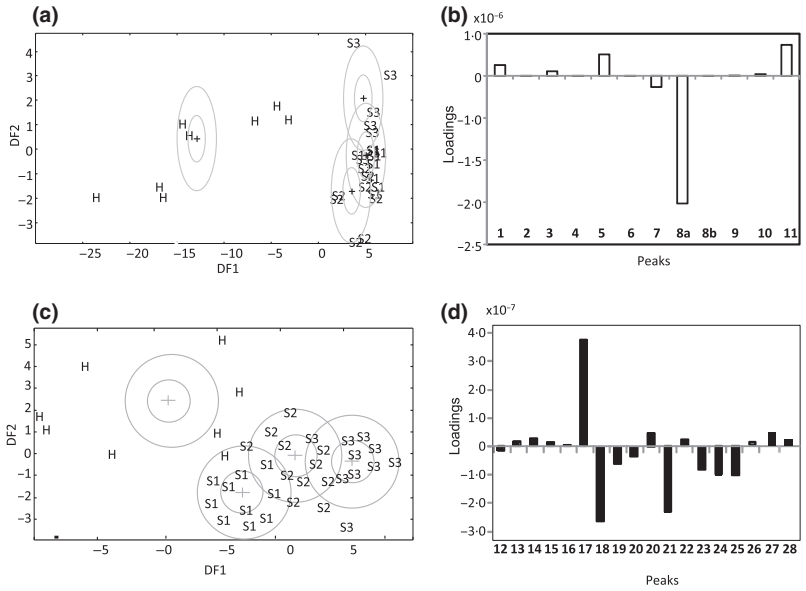

Figure 5 Infection stage-specific changes in metabolites detected in UV chromatograms at 280/340 nm from samples of tea leaves infected with blister blight. The areas of each designated peak (see Fig. 4) from HPLC-PDA (photodiode array) scans at (a) 280 nm and at (c) 340 nm were derived. Discriminant function analysis (DFA) of peak areas in spectra from healthy and tea blister infected tea leaves at designated infection stages H = healthy, S1 = stage 1, S2 = stage 2 and S3 = stage 3 were derived. DFA models were based on (a) six principal components (PC) explaining 97·45% of total variation, and (c) six PC explaining 95·24% of the total variation. The mean values are given for each class as a cross around which 90 and 95% confidence circles are shown. Associated with each DFA are loading plots for the 280 nm chromatogram (b) and for the 340 nm chromatogram (d) showing the relative importance (eigenvalues) of each peak in deriving the separations shown along each Discriminant Function 1 (DF1) axis.

prominence for peak 8A (Fig. 6b), which represented caffeine (Table 2). Examining the peak matrix from the 340 nm chromatograms, the H samples were again highly variable between sites but were distinct from infected samples (Fig. 5b). Each disease stage exhibited distinctive clustering that indicated that changes in flavonoids were prominent as infected leaves passed from S1 to S2. Plotting the DF1 loading vectors suggested that no single peak was a major source of variation between healthy and disease stage samples. However, peaks 17, 18 and 21 made the greatest contribution to variation.

To more easily view metabolite changes as blister blight developed, mean values are given in Tables S1 and S2 where differences were tested for significance. Peak areas and mean fold differences at different disease stages over H controls are displayed as heat maps (Fig. 6). Analyses of variation within replicates (here equivalent to samples from different sites) indicated that only on a single occa-

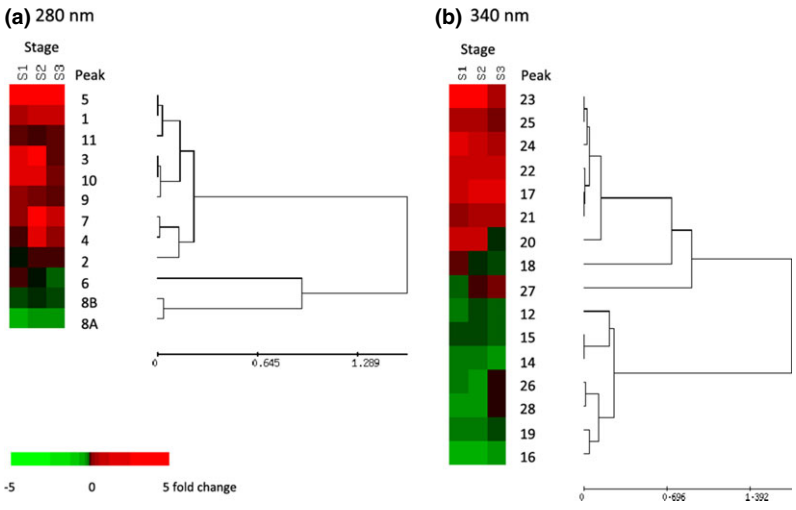

Figure 6 Heat map of changes in metabolites detected in UV chromatograms at 280/340 nm. Mean fold differences between healthy and tea blister infection stage 1 (S1), stage 2 (S2) and stage 3 (S3) derived for peaks absorbing at (a) 280 and (b) 340 nm are displayed using a heat map and compared by hierarchical cluster analyses.

sion were mean differences significant, again suggesting the reproducibility of the sampling approach. For the catechin class (metabolites detected at 280 nm), major increases following infection were suggested from the heat map (Fig. 6a), of which increases in gallate (peak 1), catechin (peak 4), epigallocatechin (peak 5), epicatechin (peak 7) and epi/gallocatechin methylgallate (peak 9) were significant (Table S1). Of the apparent reductions in metabolite content only caffeine (peak 8A), the major source of variation in Figure 5a, was significant. Similar assessment of changes in metabolites detected at 340 nm suggested both increases and decreases following infection with *E. vexan*, as shown by the heat map (Fig. 6b). However, statistically significant decreases were seen only with some of the apigenin glycosides (peaks 14B and 16A) and the myricetin glycosides (peaks 14A and 14C). Conversely, significant increases were seen with isovitexin and quercetin-*O*-hexosides (peaks 17 and 21) a kaempferol hexoside (peak 23) and co-eluting quercetin/kaempferol glucosides (peak 28) (Table S2).

Changes in jasmonic acid and salicylic acid in *E. vexans*-challenged tea

The discriminatory list (Table 1) suggested the reduction of 137 *m/z* and 179 *m/z* metabolites that were suggested to represent salicylic acid and jasmonic acid. It was also noted that *m/z* 289 and *m/z* 293, tentatively identified as 12, 13(S)-epoxylinolenate and 3-oxo-2-(cis-2′-pentenyl)-cyclopentane-1-octanoate, are jasmonate intermediates. To partially confirm these data, targeted assays for SA and JA were made on the tea samples (Fig. 7). Healthy and stage 1 samples both proved to be highly variable, with no clear trends emerging. However, in the blister-exhibiting stage 2 and necrotic stage 3 both SA and JA contents in the samples were significantly ($P < 0{\cdot}001$) reduced.

Discussion

Major threats to tea production come from climate change, pests (Hazarika *et al.*, 2009) and fungal pathogens such as *E. vexans*. Several problems hamper the implementation of effective strategies to reduce losses due to pathogens. Control of pest and pathogen most often involves the application of biocides, but their efficacy is dependent on proper use (Karthika & Muraleedharan, 2009). An alternative means of improving field resistance in tea, based on plant breeding, has been hampered by tea's domestication process. Tea is a naturally outcrossing plant so that initial production from seedlings was highly genetically heterogeneous. This led to the derivation of 'orchard varieties', which exhibited considerable variation in yield, quality and suitability for fermentation. There was then a shift to a focus on yield as the main selection criterion and a move towards clonal propagation, all of which has contributed to a relatively poor genetic variation in the tea genotype (Green, 1971; Banerjee, 1992). The aim of the current study was to assess how the tea metabolome responded to infection with *E. vexans*. This could indicate key features of disease progression, which could include defeated host defences. Crucially, these metabolomic assessments were made with infected tea samples taken from a Darjeeling plantation. To the authors' knowledge, no tea–pathogen interactions have been sampled previously under open environmental conditions, so these investigations provide a novel insight into the field responses of tea.

Fourier transform infrared spectroscopy is a well-established method through which a snapshot of sample biochemistry may be obtained (Griffiths, 1983). Analysis of the data using DFA successfully identified variation within the data sets that were associated with infection stage. Thus, the sampling approach, based on the collection of 10 separate pools of tissue, when coupled with supervised multivariate approaches (Goodacre *et al.*, 2004), allowed biologically relevant biochemical changes to be discerned. Direct infusion ESI-MS was employed to tentatively identify metabolite changes. Discriminant function analysis models suggested that three classes of metabolites appeared to be prominent: gallic acid derivatives, caffeine and flavonoids. Crucially, these metabolites were consistent with those found in studies of green tea, epicatechin

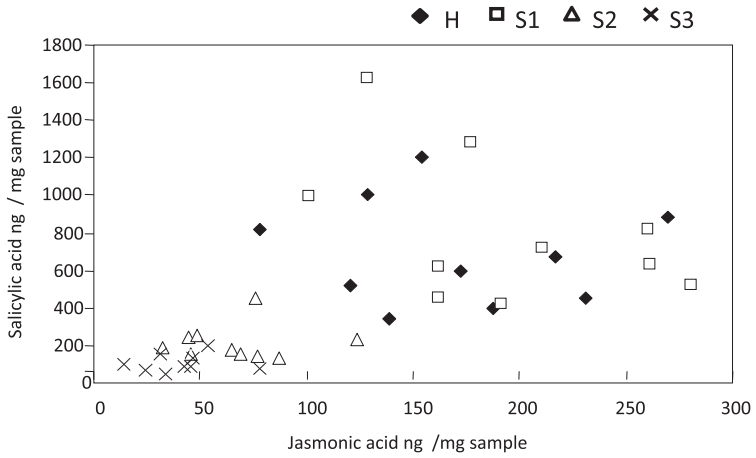

Figure 7 Salicylic and jasmonic acid content in blister blight-infected tea samples. Measurements of salicylic acid and jasmonic acid content were made of tea samples from each stage of blister blight disease; H = healthy; S1 = stage 1; S2 = stage 2; and S3 = stage 3.

with its gallate derivative and conjugates of quercetin and kaempferol (Finger *et al.*, 1992; Balentine *et al.*, 1997; Del Rio *et al.*, 2004). Even more importantly, the 'pseudo-time course' sampling approach adopted (where samples were classified according to disease stage) allowed disease-responsive changes to be suggested. These could reflect the deployment of an ultimately compromised defence response that attempts to contain or delay the progress of the pathogen. The green tea flavonols, epicatechin, epigallocatechin, epicatechin gallate, epigallocatechin gallate and gallic acid all have antioxidant activities and are known to suppress lipid peroxidation (Dai *et al.*, 2008). Such properties in green tea have been suggested to reduce the risk of cardiovascular disease and cancer (Yang & Landau, 2000). The analyses in the present study showed the accumulation of catechin-class metabolites, which could be expected to limit lipid peroxidation, a feature of several forms of disease development linked to cell death (Mur *et al.*, 2008).

A striking change occurring during disease progression was a reduction in the accumulation of the alkaloid caffeine, which was one of the most prominent sources of variation in the metabolomic analyses. Caffeine has well-established antimicrobial activity, as demonstrated by transgenic tobacco lines over-expressing three N-methyltransferases from the caffeine biosynthetic pathway (CaXMT1, CaMXMT1 and CaDXMT1). The caffeine content in these transgenic lines was in the region of 5 μg per mg fresh weight and was able to repel tobacco cutworm (*Spodoptera litura*) larvae and also *Tobacco mosaic virus* and *Pseudomonas syringae* (Kim & Sano, 2008). Thus, suppression of caffeine accumulation, possibly directly targeted by *E. vexans* pathogenic mechanisms, could be a key feature in the establishment of tea blister disease. The maintenance of caffeine levels could therefore be a target for increasing field resistance to *E. vexans*.

Caffeine production has also been linked to production of the major defence hormones SA and JA (Jia *et al.*, 2010). Therefore, it was of significance that, in the targeted assays, SA and JA content was observed to be greatly reduced by disease stage S2, a feature that will undoubtedly compromise resistance to pathogens. Thus, the SA–JA–caffeine defence network could be actively targeted by growers through the exogenous use of chemicals that initiate systemic acquired resistance (SAR) and this may potentially be an effective mechanism of reducing losses due to tea blister. Indeed, SAR activators have been shown to suppress the pathogenic fungi *Colletotrichum theae-sinensis* and *Pestalotiopsis longiseta* (Yoshida *et al.*, 2010) or the herbivorous mite *Tetranychus kanzawai* (Maeda & Ishiwari, 2012) on tea. It is also relevant that some plant growth-promoting rhizobacteria (PGPR) induce SAR (Yi *et al.*, 2013) and there has been at least one report that PGPRs are effective in reducing disease in tea (Chakraborty & Sharma, 2007). Therefore, PGPR that boost the SA–JA–caffeine pathway could be an alternative means to suppress tea blister disease in the field.

Significant increases in some glycosides of quercetin and kaempherol were observed in infected tissue. Quercetin is a potent antioxidant and has been extensively used as a therapy intervention to prevent age-associated diseases (Morel *et al.*, 1994). If quercetin glycosides are primarily acting as antioxidants in this interaction, this effect could be reduced through the significant reduction in the content of myricetin and apigenin glycosides (Table S2), which also show antioxidant activity (Hayder *et al.*, 2008; Kandasamy & Rathinam, 2011). However, quercetin, along with a range of other phenolics, can also act as a pro-oxidant to induce the peroxidase (POX)-catalysed production of H_2O_2; for example, through the use of glutathione as a redox couple (Phenolic (Ph) O + GSH + POX $\rightarrow$ $GS^{\cdot}$+ PhOH; GS + $GS^{-}\rightarrow$ $GSSG^{-}$; $GSSG^{-}$ + O_2 $\rightarrow$ O_2^{-}; O_2^{-}+ $2H^{+}\rightarrow$ H_2O_2) (Galati *et al.*, 1999). Thus, exogenous application of quercetin to *Arabidopsis* was found to enhance resistance against the bacterial pathogen *Pseudomonas syringae* pv. *tomato* (Pst) via an elevation of *in planta* H_2O_2 content and activation of salicylic mediated defences (Jia *et al.*, 2010). In a metabolomic study of grapevine (*Vitis vinifera* subsp. *vinifera*), resistance exhibited by cultivar Regent to downy and powdery mildew was tentatively linked to quercetin-3-*O*-glucoside and a *trans*-feruloyl derivative (Ali *et al.*, 2009). In an *in vitro* screen of the antifungal activity of phenolics produced by cultivated olive (*Olea europea*) against *Verticillium dahliae*-induced wilt, it was found that the aglycones quercetin and luteolin were the most potent, with catechin exhibiting relatively poor activity (Baidez *et al.*, 2007). Equally, the importance of glycosylation should not be underestimated as this augments flavonoid-influenced resistance by increasing the stability of flavonols such as kaempferol and quercetin. In flax, transgenic plants over-expressing glycosyltransferase (GT1) exhibited higher resistance to *Fusarium* infection than wildtype plants (Lorenc-Kukula *et al.*, 2009). Based on these observations, it seems likely that the increases in quercetin- and kaempferol-glycosides are part of the plant's resistance response.

Data from the metabolomics approach of this study, coupled with the pseudo-time course sampling, have provided insights into the events associated with tea blister disease progression and suggest possible agricultural targets to reduce yield losses. Thus, this work demonstrates the validity of using metabolomic strategies in open environments to monitor stress in the field.

Acknowledgements

B.N.C. acknowledges the financial support of the Royal Society of Chemistry (East India Section) in developing this project. The work of B.H. and A.W. was supported by the European Regional Development Fund, through funding provided for the BEACON project by the Welsh European Funding Office.

References

Ali K, Maltese F, Zyprian E, Rex M, Choi YH, Verpoorte R, 2009. NMR metabolic fingerprinting based identification of grapevine

metabolites associated with downy mildew resistance. *Journal of Agricultural & Food Chemistry* **57**, 9599–606.
Allwood JW, Ellis DI, Heald JK, Goodacre R, Mur LAJ, 2006. Metabolomic approaches reveal that phosphatidic and phosphatidyl glycerol phospholipids are major discriminatory non-polar metabolites in responses by *Brachypodium distachyon* to challenge by *Magnaporthe grisea*. *The Plant Journal* **46**, 351–68.
Aron PM, Kennedy JA, 2008. Flavan-3-ols: nature, occurrence and biological activity. *Molecular Nutrition & Food Research* **52**, 79–104.
Atoui AK, Mansouri A, Boskou G, Kefalas P, 2005. Tea and herbal infusions: their antioxidant activity and phenolic profile. *Food Chemistry* **89**, 27–36.
Baidez AG, Gomez P, Del Rio JA, Ortuno A, 2007. Dysfunctionality of the xylem in *Olea europaea* L. plants associated with the infection process by *Verticillium dahliae* Kleb. Role of phenolic compounds in plant defense mechanism. *Journal of Agricultural & Food Chemistry* **55**, 3373–7.
Balasooriya J, 1996. Effect of altitude on shoot development of clonal tea with special reference to clonal selection and harvesting intervals. *Sri Lankan Journal of Tea Science* **64**, 51–62.
Balentine DA, Wiseman SA, Bouwens LC, 1997. The chemistry of tea flavonoids. *Critical Reviews in Food Science & Nutrition* **37**, 693–704.
Banerjee B, 1992. Selection and breeding criteria. In: Willson KC, Clifford MN, eds. *Tea: Cultivation to Consumption*. London, UK: Chapman and Hall, 53–81.
Boekhout T, 1991. A revision of ballistoconidia-forming yeasts and fungi. *Studies in Mycology* **33**, 1–194.
Brazma A, Parkinson H, Sarkans U *et al.*, 2003. ArrayExpress – a public repository for microarray gene expression data at the EBI. *Nucleic Acids Research* **31**, 68–71.
Chakraborty BN, Sharma M, 2007. Serological detection and immunogold localization of cross-reactive antigens shared by *Camellia sinensis* and *Exobasidium vexans*. *Journal of Applied Microbiology* **103**, 1669–80.
Clarke SM, Mur LAJ, Wood JE, Scott IM, 2004. Salicylic acid dependent signaling promotes basal thermotolerance but is not essential for acquired thermotolerance in *Arabidopsis thaliana*. *The Plant Journal* **38**, 432–47.
Dai F, Chen WF, Zhou B, 2008. Antioxidant synergism of green tea polyphenols with alpha-tocopherol and L-ascorbic acid in SDS micelles. *Biochimie* **90**, 1499–505.
Del Rio D, Stewart AJ, Mullen W *et al.*, 2004. HPLC-MS^n analysis of phenolic compounds and purine alkaloids in green and black tea. *Journal of Agricultural & Food Chemistry* **52**, 2807–15.
Dou JP, Lee VSY, Tzen JTC, Lee MR, 2007. Identification and comparison of phenolic compounds in the preparation of oolong tea manufactured by semifermentation and drying processes. *Journal of Agricultural & Food Chemistry* **55**, 7462–8.
Evensen NA, Braun PC, 2009. The effects of tea polyphenols on *Candida albicans*: inhibition of biofilm formation and proteasome inactivation. *Canadian Journal of Microbiology* **55**, 1033–9.
FAOSTAT, 2010. Food and Agriculture Organization of the United Nations – Production FAOSTAT. [http://faostat.fao.org/site/567/default.aspx#ancor FAOSTAT]. Accessed 10 September 2010.
Ferreres F, Silva BM, Andrade PB, Seabra RM, Ferreira MA, 2003. Approach to the study of *C*-glycosyl flavones by ion trap HPLC-PAD-ESI/MS/MS: application to seeds of quince (*Cydonia oblonga*). *Phytochemical Analysis* **14**, 352–9.
Ferreres F, Gil-Izquierdo A, Andrade PB, Valentao P, Tomas-Barberan FA, 2007. Characterization of *C*-glycosyl flavones *O*-glycosylated by liquid chromatography-tandem mass spectrometry. *Journal of Chromatography A* **1161**, 214–23.
Ferreres F, Andrade PB, Valentao P, Gil-Izquierdo A, 2008. Further knowledge on barley (*Hordeum vulgare* L.) leaves *O*-glycosyl-*C*-glycosyl flavones by liquid chromatography-UV diode-array detection-electrospray ionisation mass spectrometry. *Journal of Chromatography A* **1182**, 56–64.
Finger A, Engelhardt UH, Wray V, 1991. Flavonol glycosides in tea – kaempferol and quercetin rhamnodiglucosides. *Journal of the Science of Food & Agriculture* **55**, 313–21.
Finger A, Kuhr S, Engelhardt UH, 1992. Chromatography of tea constituents. *Journal of Chromatography* **624**, 293–315.
Friedman M, Kim SY, Lee SJ *et al.*, 2005. Distribution of catechins, theaflavins, caffeine, and theobromine in 77 teas consumed in the United States. *Journal of Food Science* **70**, C550–9.
Galati G, Chan T, Wu B, O'Brien PJ, 1999. Glutathione-dependent generation of reactive oxygen species by the peroxidase-catalyzed redox cycling of flavonoids. *Chemical Research in Toxicology* **12**, 521–5.
Goodacre R, Vaidyanathan S, Dunn WB, Harrigan GG, Kell DB, 2004. Metabolomics by numbers: acquiring and understanding global metabolite data. *Trends in Biotechnology* **22**, 245–52.
Goodacre R, Broadhurst D, Smilde AK *et al.*, 2007. Proposed minimum reporting standards for data analysis in metabolomics. *Metabolomics* **3**, 231–41.
Gordon NC, Wareham DW, 2010. Antimicrobial activity of the green tea polyphenol (–)-epigallocatechin-3-gallate (EGCG) against clinical isolates of *Stenotrophomonas maltophilia*. *International Journal of Antimicrobial Agents* **36**, 129–31.
Green MJ, 1971. An evaluation of some criteria used in selecting large-yielding tea clones. *Journal of Agricultural Science* **76**, 143.
Griffiths PR, 1983. Fourier-transform infrared spectrometry. *Science* **222**, 297–302.
Hayder N, Bouhlel I, Skandrani I *et al.*, 2008. *In vitro* antioxidant and antigenotoxic potentials of myricetin-3-*O*-galactoside and myricetin-3-*O*-rhamnoside from *Myrtus communis:* modulation of expression of genes involved in cell defence system using cDNA microarray. *Toxicology in Vitro* **22**, 567–81.
Hazarika LK, Bhuyan M, Hazarika BN, 2009. Insect pests of tea and their management. *Annual Review of Entomology* **54**, 267–84.
Jarvis RM, Broadhurst D, Johnson H, O'Boyle NM, Goodacre R, 2006. PYCHEM: a multivariate analysis package for python. *Bioinformatics* **22**, 2565–6.
Jeyaramraja PR, Pius PK, Manian S, Meenakshi SN, 2005. Certain factors associated with blister blight resistance in *Camellia sinensis* (L.) O. *Kuntze*. *Physiological and Molecular Plant Pathology* **67**, 291–5.
Jia ZH, Zou BH, Wang XM *et al.*, 2010. Quercetin-induced H_2O_2 mediates the pathogen resistance against *Pseudomonas syringae* pv. *tomato* DC3000 in *Arabidopsis thaliana*. *Biochemical & Biophysical Research Communications* **396**, 522–7.
Johnson HE, Broadhurst D, Goodacre R, Smith AR, 2003. Metabolic fingerprinting of salt-stressed tomatoes. *Phytochemistry* **62**, 919–28.
Johnson HE, Lloyd AJ, Mur LAJ, Smith AR, Causton DR, 2007. The application of MANOVA to analyse *Arabidopsis thaliana* metabolomic data from factorially designed experiments. *Metabolomics* **3**, 517–30.
Kandasamy S, Rathinam K, 2011. A comparative DFT study on the antioxidant activity of apigenin and scutellarein flavonoid compounds. *Molecular Physics* **109**, 839–52.
Karthika C, Muraleedharan NN, 2009. Contribution of leaf growth on the disappearance of fungicides used on tea under south Indian agroclimatic conditions. *Journal of Zhejiang University Science B* **10**, 422–6.
Kiehne A, Engelhardt UH, 1996a. Thermospray-LC-MS analysis of various groups of polyphenols in tea. 1. Catechins, flavonol *O*-glycosides and flavone *C*-glycosides. *Zeitschrift für Lebensmittel-Untersuchung und -Forschung* **202**, 48–54.
Kiehne A, Engelhardt UH, 1996b. Thermospray-LC-MS analysis of various groups of polyphenols in tea. 2. Chlorogenic acids, theaflavins and thearubigins. *Zeitschrift für Lebensmittel-Untersuchung und -Forschung* **202**, 299–302.
Kiehne A, Lakenbrink C, Engelhardt UH, 1997. Analysis of proanthocyanidins in tea samples.1. LC-MS results. *Zeitschrift für Lebensmittel-Untersuchung und -Forschung* **205**, 153–7.
Kim YS, Sano H, 2008. Pathogen resistance of transgenic tobacco plants producing caffeine. *Phytochemistry* **69**, 882–8.

Lee VSY, Chen CR, Liao YW, Tzen JTC, Chang CI, 2008. Structural determination and DPPH radical-scavenging activity of two acylated flavonoid tetraglycosides in oolong tea (*Camellia sinensis*). *Chemical & Pharmaceutical Bulletin* **56**, 851–3.

Lin LZ, Chen P, Harnly JM, 2008. New phenolic components and chromatographic profiles of green and fermented teas. *Journal of Agricultural & Food Chemistry* **56**, 8130–40.

Lorenc-Kukula K, Zuk M, Kulma A *et al.*, 2009. Engineering lax with the GT Family 1 *Solanum sogarandinum* glycosyltransferase SsGT1 confers increased resistance to *Fusarium* infection. *Journal of Agricultural & Food Chemistry* **57**, 6698–705.

Lu JL, Wang DM, Shi XG, Yang DP, Zheng XQ, Ye CX, 2009. Determination of purine alkaloids and catechins in different parts of *Camellia assamica* var. *kucha* by HPLC-DAD/ESI-MS/MS. *Journal of the Science of Food & Agriculture* **89**, 2024–9.

Maeda T, Ishiwari H, 2012. Tiadinil, a plant activator of systemic acquired resistance, boosts the production of herbivore-induced plant volatiles that attract the predatory mite *Neoseiulus womersleyi* in the tea plant *Camellia sinensis*. *Experimental and Applied Acarology* **58**, 247–58.

Markby TJ, Markham KR, Thomas BT, 1970. *The Systemic Identification of Flavonoids*. New York, USA: Springer-Verlag.

Martosupono M, 1991. Some factors influenced the tea resistance to blister blight. In: Yamanishi T, ed. *Proceedings of the International Symposium on Tea Science, 1991*. Shizuoka, Japan: ISTS, 651–4.

Mattoli L, Cangi F, Maidecchi A *et al.*, 2006. Metabolomic fingerprinting of plant extracts. *Journal of Mass Spectrometry* **41**, 1534–45.

Morel I, Lescoat G, Cillard P, Cillard J, 1994. Role of flavonoids and iron chelation in antioxidant action. *Oxygen Radicals in Biological Systems, Part D* **234**, 437–43.

Mur LAJ, Kenton P, Lloyd AJ, Ougham H, Prats E, 2008. The hypersensitive response; the centenary is upon us but how much do we know? *Journal of Experimental Botany* **59**, 501–20.

Nagahaulla KSM, Herath N, Punyasiri N, 1996. A preliminary study of the phytoalexins produced in the tea leaf in relation to the blister blight leaf disease caused by *Exobasidium vexans* Massee of tea. *Sri Lanka Journal of Tea Science* **64**, 5–11.

Park KD, Park YS, Cho SJ *et al.*, 2004. Antimicrobial activity of 3-*O*-acyl-(–)-epicatechin and 3-*O*-acyl-(+)-catechin derivatives. *Planta Medica* **70**, 272–6.

Pius PK, Krishnamurthy KV, Nelson R, 1998. Changes in saccharide metabolism induced by infection of *Camellia sinensis* by *Exobasidium vexans*. *Biologia Plantarum* **41**, 127–32.

Premkumar R, Baby UI, 2005. Blister blight control – a review of current recommendations. *Journal of Plantation Crops* **101**, 26–34.

Punyasiri PA, Abeysinghe SB, Kumar V, 2005. Preformed and induced chemical resistance of tea leaf against *Exobasidium vexans* infection. *Journal of Chemical Ecology* **31**, 1315–24.

Radhakrishnan B, Baby UI, 2004. Economic threshold level for blister blight of tea. *Indian Phytopathology* **57**, 195–6.

Rajalakshmi N, Ramarethinam S, 2000. The role of *Exobasidium vexans* Massee in flavanoid synthesis by *Camellia assamica* Shneider. *Indian Journal of Plant Protection* **28**, 1–8.

Sano M, Suzuki M, Miyase T, Yoshino K, Maeda-Yamamoto M, 1999. Novel antiallergic catechin derivatives isolated from oolong tea. *Journal of Agricultural & Food Chemistry* **47**, 1906–10.

Santos-Buelga C, García-Viguera C, Tomás-Barberán FA, 2003. On-line identification of flavonoids by HPLC coupled to diode array detection. In: Celestino Santos-Buelga C, Williamson G, eds. *Methods in Polyphenol Analysis*. Cambridge, UK: Royal Society of Chemistry (Great Britain), 92–127.

Saracini E, Tattini M, Traversi ML, Vincieri FF, Pinelli P, 2005. Simultaneous LC-DAD and LC-MS determination of ellagitannins, flavonoid glycosides, and acyl-glycosyl flavonoids in *Cistus salvifolius* L. leaves. *Chromatographia* **62**, 245–9.

Sitheeque MAM, Panagoda GJ, Yau J, Amarakoon AMT, Udagama URN, Samaranayake LP, 2009. Antifungal activity of black tea polyphenols (catechins and theaflavins) against *Candida* species. *Chemotherapy* **55**, 189–96.

Song JM, Seong BL, 2007. Tea catechins as a potential alternative anti-infectious agent. *Expert Review of Anti-Infective Therapy* **5**, 497–506.

Timmins EM, Howell SA, Alsberg BK, Noble WC, Goodacre R, 1998. Rapid differentiation of closely related *Candida* species and strains by pyrolysis mass spectrometry and Fourier transform-infrared spectroscopy. *Journal of Clinical Microbiology* **36**, 367–74.

Vidhyasekaran P, 1988. *Physiology of Disease Resistance in Plants*. Boca Raton, FL, USA: CRC Press.

Vukics V, Guttman A, 2010. Structural characterization of flavonoid glycosides by multi-stage mass spectrometry. *Mass Spectrometry Reviews* **29**, 1–16.

Wang DM, Lu JL, Miao AQ, Xie ZY, Yang DP, 2008. HPLC-DAD-ESI-MS/MS analysis in leaves of 22 tea of polyphenols and purine alkaloids cultivars in China. *Journal of Food Composition and Analysis* **21**, 361–9.

Wu W, Yan CY, Li L, Liu ZQ, Liu SY, 2004. Studies on the flavones using liquid chromatography-electrospray ionization tandem mass spectrometry. *Journal of Chromatography A* **1047**, 213–20.

Yang CS, Landau JM, 2000. Effects of tea consumption on nutrition and health. *Journal of Nutrition* **130**, 2409–12.

Yi HS, Yang JW, Ryu CM, 2013. ISR meets SAR outside: additive action of the endophyte *Bacillus pumilus* INR7 and the chemical inducer, benzothiadiazole, on induced resistance against bacterial spot in field-grown pepper. *Frontiers in Plant Science* **4**, 122.

Yoshida K, Ogino A, Yamada K, Sonoda R, 2010. Induction of disease resistance in tea (*Camellia sinensis* L.) by plant activators. *Japan Agricultural Research Quarterly* **44**, 391–8.

Supporting Information

Additional Supporting Information may be found in the online version of this article at the publisher's web-site.

Figure S1. Metabolites within the caffeine biosynthetic pathway that may be prominent amongst the key changes in tea blister blight samples.

Figure S2. Flavanoid metabolites that are prominent amongst the key changes in tea blister blight samples.

Figure S3. Site-specific differences in flavonols in tea samples.

Table S1. Testing for disease stage-associated significant differences in peak areas in UV/vis chromatograms for metabolites detected at 280 nm in samples infected with tea blister blight.

Table S2. Testing for disease stage-associated significant differences in peak areas in UV/vis chromatograms for metabolites detected at 340 nm in samples infected with tea blister blight